Short Silk Fiber-Reinforced Polychloroprene Rubber Composites

D. K. SETUA and B. DUTTA*, *Rubber Technology Centre, Indian Institute of Technology, Kharagpur 721302, India*

Synopsis

The reinforcement of polychloroprene rubber by short silk fiber has been studied in the presence of three different dry bonding systems, viz.: (a) "cohedur RK–cohedur A–silica"; (b) "cohedur RK–cohedur A–carbon black"; (c) "resorcinol–hexamethylenetetramine–silica." The degree of fiber–rubber adhesion of the different bonding systems follows the order (a) > (b) > (c). Scanning electron microscopy studies of tensile, tear, abrasion, and flex failed surfaces of both unfilled and fiber–filled composites containing "cohedur–silica" bonding system have also been made in order to gain an insight to the mechanism of failure.

INTRODUCTION

Lately, short fiber-reinforced rubber has gained importance due to its advantages such as design flexibility, higher low strain moduli, anisotropy in technical properties, stiffness, damping, and processing economy.[1-9] Short fiber reinforcement in the production of hoses, V-belts, tire treads, spindle drive wheel, and complex-shaped mechanical goods have been studied by many workers.[10-21] Investigations have also been made on the feasibility of using rubber/fiber compositions, obtained from various types of waste from rubberized materials and cord, in the production of V-belts and tire tread compounds.[22-24] The extent of reinforcement has been found to depend on the fiber–matrix adhesion, aspect ratio of the fiber in the vulcanizate, fiber dispersion and orientation, nature of the matrix, and type of fiber.[25-30] Recently, Setua and De have reported their studies on short silk fiber reinforcement of natural and nitrile rubbers.[31,32]

Since both silk and polychloroprene are polar, good fiber–rubber adhesion is expected. In the present paper, we report results of our investigations on short silk fiber reinforcement of polychloroprene rubber.

It has been reported earlier that the presence of tricomponent dry bonding system (e.g., resorcinol–hexamethylenetetramine–silica) is essential for the promotion of adhesion between the fiber and rubber matrix.[9,31-35] Recently, some researchers have found that the replacement of silica by carbon black in the tricomponent dry bonding system leads to essentially similar adhesion level.[36,37] It is interesting, therefore, to study how the relative efficiencies of silica or carbon black at a constant loading affect the reinforcement characteristics in short fiber–rubber systems. Our studies can be divided into the following parts: (i) effect of different bonding systems on the technical properties and processing characteristics of the mixes; (ii) effect of the

* Bengal Waterproof Ltd., Panihati, West Bengal, India.

Journal of Applied Polymer Science, Vol. 29, 3097–3114 (1984)
 CCC 0021-8995/84/103097-18$04.00

concentrations of bonding agents on fiber–rubber adhesion; and (iii) anisotropy in the technical properties of fiber–rubber composites.

Scanning electron microscopy (SEM) studies of the tensile, tear, flexing, and abrasion failed surfaces have also been made in order to gain an insight to the mechanism of failure.

EXPERIMENTAL

Waste silk fiber was first separated from undesirable foreign matter and chopped to 6 mm length. Mixing was done on a conventional laboratory open mill (150 mm × 330 mm) at 30–40°C according to ASTM designation D 15-70. Nip gap, mill roll speed ratio, time of mixing, and the sequence of addition of the ingredients (as shown in Tables I and IV) were kept the same for all the mixes. Shear force during mixing oriented most of the fibers along the grain direction (Figs. 9 and 12), but this also caused fiber breakage. Extent of fiber breakage was studied by dissolving the compounds in chloroform, followed by extraction of the fibers and examination of fiber length distribution by a optical polarizing microscope (model Leitz HM-Pol) under reflected light.

Extent of fiber breakage during mixing is not affected by the different bonding systems and the fall in the mean aspect ratio from its original value of 500 to 85 after mixing is almost the same for all the mixes. A general breakage pattern of the fibers after mixing is shown in Figure 1. No change in the average diameter (0.012 mm) of the fiber occurred during mixing.

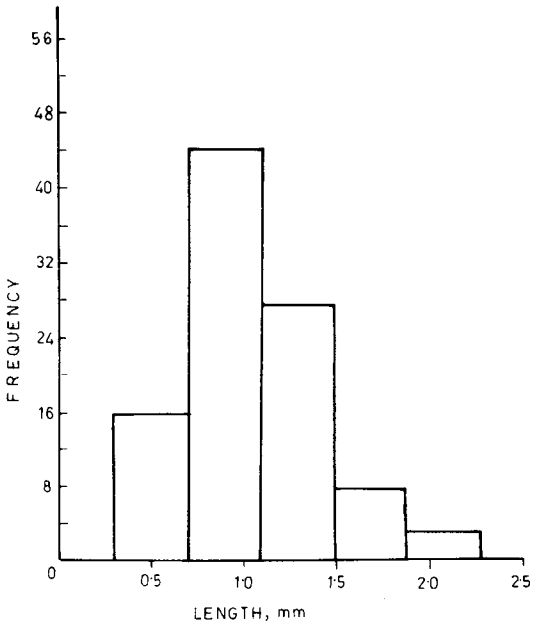

Fig. 1. Distribution of length of the broken fibers after mixing as obtained with the polarizing microscope.

Mixes were vulcanized to their respective optimum cure times as determined by Monsanto rheometer R-100, at 150°C and 4.5 N · mm^{-2} pressure in a hydraulic press. The details of the preparation of vulcanizates have been described in a previous publication.[38] Stress–strain properties were determined by using Instron Universal Testing Machine (Model 1195) at a crosshead speed of 500 mm/min.

Tensile, tear, flexing, heat buildup, abrasion, hardness, and compression sets were measured according to ASTM procedures. Resilience was determined at 35°C by using a Dunlop tripsometer according to BS 903 part-2, 1950. Tests like tensile, tear, abrasion, flexing, compression sets, and heat buildup were carried out, both along (that is, longitudinally oriented fibers) and across (that is, transversely oriented fibers) the grain direction. Resilience and hardness measurements were made with tensile sheet specimens and orientation of the fibers in these cases was normal to the direction of the application of the load.

Figures 2 and 3 show the shapes of the tensile and tear test specimens with longitudinally and transversely oriented fibers, and the corresponding fractured surfaces and scan areas. Figure 4 shows the fiber directionality in the test specimens of abrasion and flexing tests. The portion of the specimens used for SEM studies has also been shown. The axes of the test geometry with reference to fiber directionality in the cases of compression

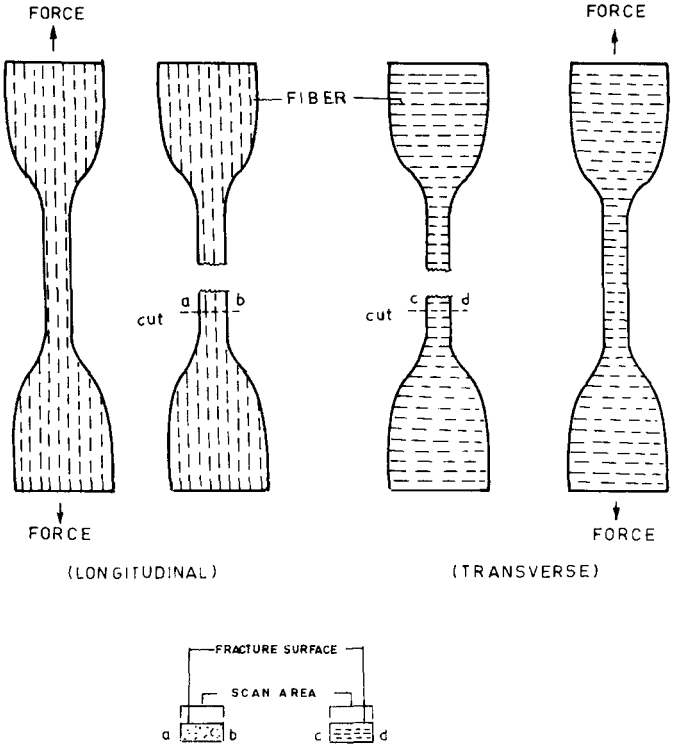

Fig. 2. Shapes of the tensile test specimens with longitudinal and transverse fiber orientation, corresponding fractured surfaces and scan areas.

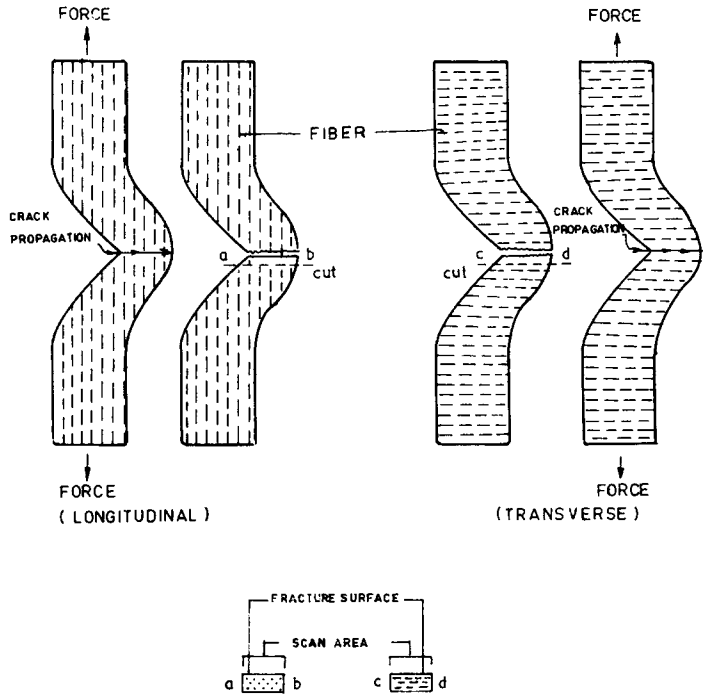

Fig. 3. Shapes of the tear test specimens with longitudinal and transverse fiber orientation, corresponding fractured surfaces and scan areas.

set, heat buildup, resilience, and hardness test samples are depicted in Figure 5. The fracture surfaces were sputter-coated with gold within 24 h of testing. SEM studies were carried out using a Philips Model 500 Scanning Electron Microscope. The orientation of the photographs was kept constant for a particular mode of testing and the tilt was adjusted to 0° in all cases.

Methods of determination of the volume fraction of rubber in the solvent swollen vulcanizate (V_r) and the processing characteristics like mill shrinkage, Mooney viscosity ML (1 + 4), Mooney scorch time, and the green strength of the compounds have been described earlier.[31,32]

RESULTS AND DISCUSSION

Role of Bonding Agents in the Adhesion between the Fiber and the Rubber

Formulations of the mixes and the technical properties of the vulcanizates are given in Tables I and II, respectively. Mix A does not contain any bonding agent, mix B does not contain silica in the cohedur bonding system, mix C contains an insufficient level (5 phr) of silica, and mix D contains optimum proportion (10 phr) of silica in the bonding system. Mix E contains "resorcinol–hexamethylenetetramine–silica" bonding system in place of "cohedur–silica" bonding system. It is evident from Table II that due to poor fiber–rubber adhesion (e.g., for mixes A, B, and C), the test specimens in the

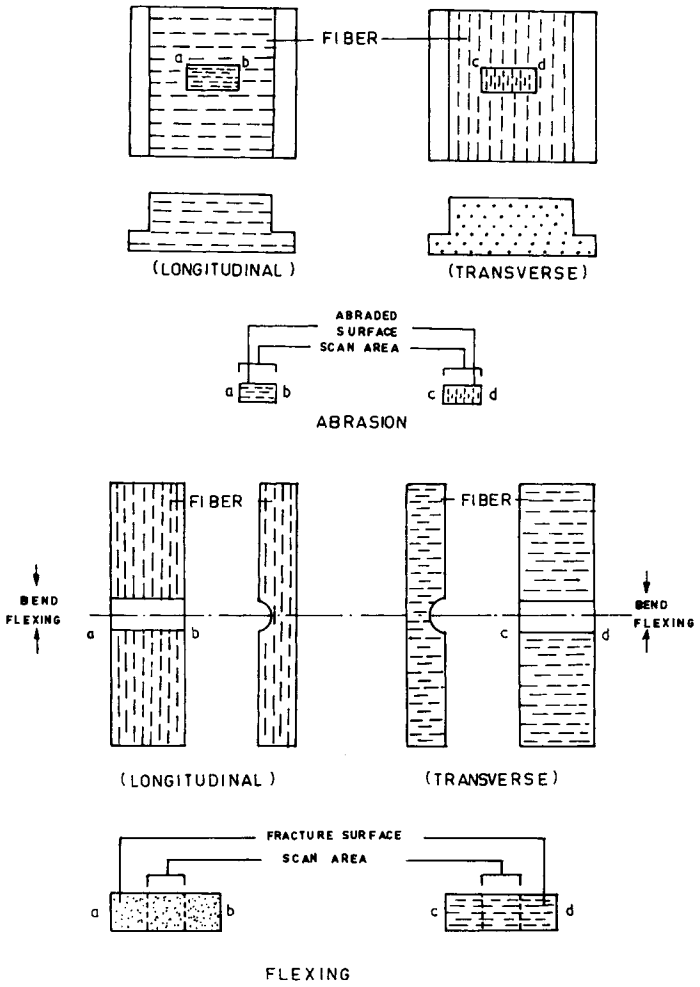

Fig. 4. Fiber directionality and scan areas in the test specimens of abrasion and De Mattia flexing tests.

Goodrich flexometer testing could not withstand dynamic compression and failed at a much earlier stage as compared to mix D. Improvement in the adhesion level is also reflected in the tensile strength, elongation at break, and compression set (both at constant stress and at constant strain) properties of the vulcanizates which are found to improve gradually from mixes A–D. Due to lower elongation at break values for all the mixes with longitudinal fiber orientation, the matrix itself does not provide any resistance to tearing. The tear strength in this orientation depends mainly on the concentration of fibers which resists the growth of the tear by deflecting the tear path from proceeding straight and is independent of the degree of adhesion between the fiber and the matrix. Mixes A–D, therefore, show similar tear strength. However, in the transverse orientation, resistance offered by the fibers is less as the fracture path moves parallel to the direction of orientation of fibers. The fiber and the matrix, in this case,

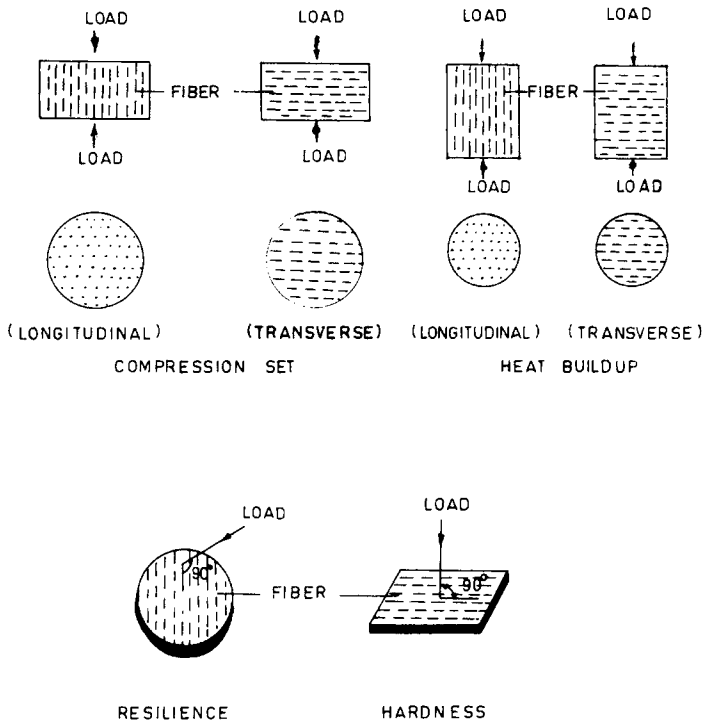

Fig. 5. Fiber directionality in the test specimens of compression set, heat buildup, resilience, and hardness tests.

constitute one system, and tear strength depends on the tearing energy of the composites, which, in turn, depends on the degree of adhesion between the fiber and the matrix. Thus in transverse orientation, gradual increase in tear strength from mixes A–D is observed. This is similar to our previous observation.[31,32]

In the case of short silk fiber-reinforced natural and nitrile rubber composites "resorcinol–hexamethylenetetramine–silica" bonding system was found to be effective as far as technical properties and processing characteristics are considered.[31,32] With this view in mind, mix E containing this bonding system was included. A comparison between mixes E and D showed that the former lead to a lower tensile strength, tear strength (transverse fiber orientation), elongation at break, and anisotropy in the technical properties but higher compression set (at both constant stress and constant strain) and heat buildup implying thereby a lower level of fiber–rubber adhesion in mix E compared to that in mix D. Processing characteristics of mix E (as shown in Table III) are also inferior to those of mix D. Faster curing due to the presence of resorcinol and hexamethylenetetramine in mix E leads to drastic reductions in optimum cure time and Mooney scorch time and causes a lower level of adhesion between the fiber and the rubber matrix. Hence the use of "cohedur RK–cohedur A–silica" bonding system, which provides an optimum set of physical properties and processing characteristics, is preferred to "resorcinol–hexamethylenetetramine–silica" system in silk–polychloroprene rubber composites.

TABLE I
Formulation of Mixes

Parameter	Content of mix (parts by weight)				
	A	B	C	D	E
Polychloroprene[a]	100	100	100	100	100
MgO[b]	4	4	4	4	4
PBNA[c]	2	2	2	2	2
Silica[d]	—	—	5	10	10
Silk fiber[e]	20	20	20	20	20
Stearic acid	0.5	0.5	0.5	0.5	0.5
Resorcinol	—	—	—	—	5
Cohedur RK[f]	—	5	5	10	—
ZnO	5	5	5	5	5
Cohedur A[g]	—	1.6	1.6	3.2	—
Hexamethylenetetramine	—	—	—	—	3.2
TMTM[h]	1	1	1	1	1
DOTG[i]	0.5	0.5	0.5	0.5	0.5
Sulfur	0.5	0.5	0.5	0.5	0.5

[a] Neoprene, WM-1 grade, supplied by Bengal Waterproof Ltd., Panihati, Calcutta.

[b] Magnesia, neoprene grade, supplied by Bengal Waterproof Ltd., Panihati, Calcutta.

[c] Phenyl β-naphthylamine (Accinox DN), supplied by Alkali and Chemical Corporation of India Ltd., Rishra.

[d] Vulcasil-S, supplied by Bata India Ltd., Calcutta.

[e] Mulberry type of silk fiber, obtained in filatures of Silk Khadi Mondol, Bishnupur, West Bengal.

[f] A condensation product of resorcinol and formaldehyde, obtained from Bayer India Ltd., Bombay.

[g] Methoxymethyl melamine, obtained from Bayer India Ltd., Bombay.

[h] Tetramethylthiuram monosulfide, supplied by Alkali and Chemical Corporation of India Ltd., Rishra.

[i] Diortho-tolyl guanidine, supplied by Bengal Waterproof Ltd., Panihati, Calcutta.

TABLE II
Technical Properties of Vulcanizates

Property	Fiber orientation[a]	Vulcanizate				
		A	B	C	D	E
Optimum cure time at 150°C (min)	—	34.0	28.0	29.0	31.5	14.0
Hardness (Shore A)	—	85	87	89	92	88
Tear strength (kN/m)	L	42.4	43.0	44.0	46.6	41.8
	T	34.0	39.6	43.8	59.9	38.8
Tensile strength (MPa)	L	7.78	8.21	8.74	11.45	9.32
	T	4.59	5.03	6.13	6.45	5.58
Elongation at break (%)	L	48	45	65	25	35
	T	110	465	420	380	125
Compression set at constant strain (25%) (%)	L	59	53	50	42	52
	T	57	49	47	39	50
Compression set at constant stress (400 lb) (%)	L	11	10	9	7	10
	T	14	12	11	9	12
Heat buildup (ΔT) at 50°C (°C)[b]	L	28(5)	34(9)	38(12)	41(18)	45(16)
	T	16(2)	38(7)	40(10)	44(15)	47(85)

[a] L denotes longitudinal and T denotes transverse orientation.

[b] Values in the parentheses indicate time (min) of failure of the test specimens.

TABLE III
Processing Characteristics of the Mixes

Property	Fiber orientation	Mix D (cohedur–silica bonding system)	Mix E (resorcinol–hexamethylenetetramine–silica bonding system)
Mill shrinkage (%)	—	2.0	3.5
Mooney viscosity ML (1 + 4), at 120°C	—	49.5	62.0
Mooney scorch time T_5 at 120°C (min)	—	11.5	3.5
Green strength (MPa)	L	2.72	2.35
	T	0.55	0.41

Relative Efficiencies of Silica and Carbon Black as an Essential Parameter in the Tricomponent Dry Bonding System

Formulation of mixes D, F, and G and technical properties of the vulcanizates are furnished in Tables IV and V, respectively. Figure 6 shows the stress–strain curves of the mixes. Mix F is similar to mix D with carbon black in place of silica. Mix G is the corresponding gum mix without fiber and bonding agents.

While no significant changes in the optimum cure times were observed due to addition of fibers in the mixes, their presence in mixes D and F leads to a drastic reduction in the elongation at break values and simultaneous

TABLE IV
Formulation of Mixes

Parameter	Content of mix (parts by weight) D	F	G
Polychloroprene	100	100	100
MgO	4	4	4
PBNA	2	2	2
Silica	10	—	—
Carbon black[a]	—	10	—
Processing oil	—	1	—
Silk fiber	20	20	—
Stearic acid	0.5	0.5	0.5
Cohedur RK	10	10	—
ZnO	5	5	5
Cohedur A	3.2	3.2	—
TMTM	1	1	1
DOTG	0.5	0.5	0.5
Sulfur	0.5	0.5	0.5

[a] Semireinforcing carbon black (FEF-N550), supplied by Phillips Carbon Black Ltd., Durgapur.

TABLE V
Technical Properties of Vulcanizates

Property	Fiber orientation	Vulcanizate D	Vulcanizate F	Vulcanizate G
Optimum cure time at 150°C (min)	—	31.5	30.0	34.0
Hardness (Shore A)	—	92	90	50
Tear strength (kN/m)	L	46.6	43.0	21.5
	T	59.9	51.2	
Tensile strength (MPa)	L	11.45	9.61	14.85
	T	6.45	8.19	
Elongation at break (%)	L	25	30	910
	T	380	450	
Compression set at constant strain (25%) (%)	L	42	46	35
	T	39	44	
Compression set at constant stress (400 lb) (%)	L	7	9	15
	T	9	10	
Heat buildup (ΔT) at 50°C (°C)	L	41(18)	39(15)	21[a]
	T	44(15)	46(13)	
Rebound resilience (%)	—	55	53	69
Abrasion loss (mL/h)	L	1.83	1.98	4.19
	T	1.69	1.75	
Flex cracking resistance (k cycles)	L	3.1	2.2	8.5
	T	4.2	3.7	
Modulus at 25% elongation (MPa)	L	11.45	8.42	—
	T	2.62	4.52	
V_r[b]	—	0.299	0.278	0.138

[a] The sample did not fail and the heat buildup value was taken after 20 min of flexing.
[b] Chloroform was used as the solvent.

increase in the low elongation (25%) modulus in both orientations, unlike mix G. Higher values for elongation at break in the transverse orientation of fibers are observed for mixes D and F. Modulus at 25% elongation shows the reverse trend; that is, higher modulus is observed in the longitudinal orientation than in the transverse orientation. The tensile strength of mixes D and F depends primarily on the fibers which obstruct the progress of the fracture front. Breakage and pulling out of the fibers take place when the fibers are oriented longitudinally (i.e., perpendicular to the fracture direction), whereas for transversely oriented fibers the crack progresses in the direction of fiber alignment, experiencing, therefore, a lower resistance by the fibers. Hence the tensile strength of composites with longitudinal fiber orientation is always higher than that of composites with transverse fiber orientation.

Figure 7 is the SEM photomicrograph of the tensile-fractured surface of unfilled vulcanizate of mix G. It shows the presence of a rough zone at one edge of the fracture surface preceded by a comparatively smooth region consisting of many short tear lines. Fiber-filled composites (mix D) exhibit a marked change in the fracture topography. Due to increased hardness, the composites become brittle, which results in the development of deep

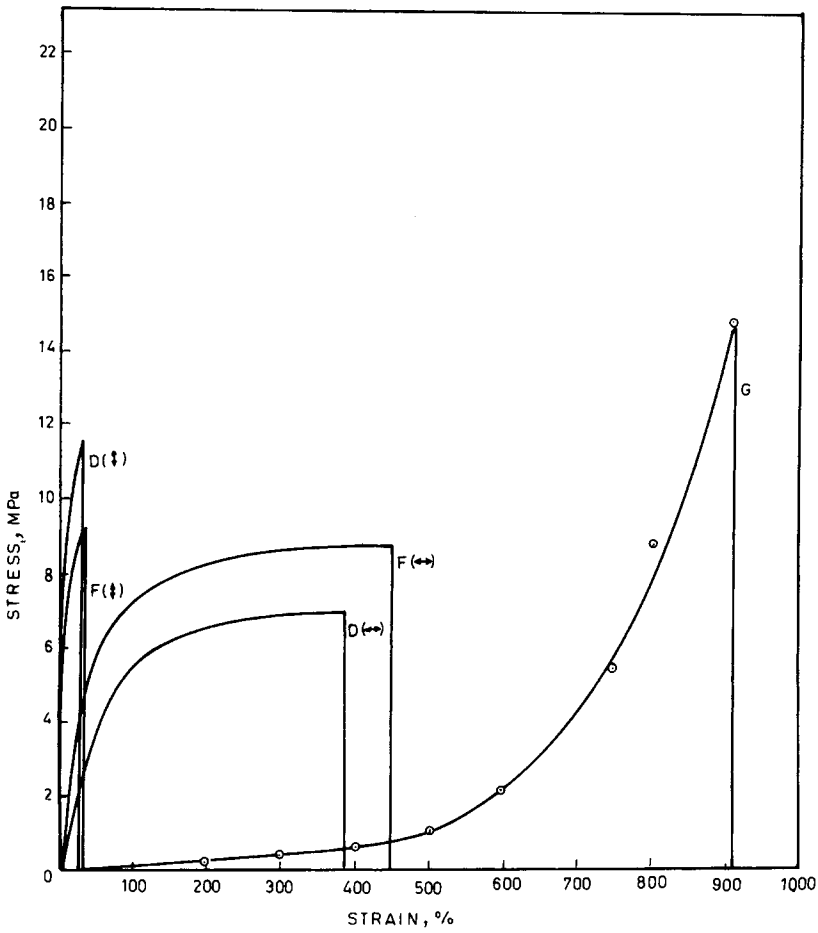

Fig. 6. Stress–strain curves of the mixes D, F, and G; fibers oriented longitudinally (↕) and transversely (↔) in mixes D and F.

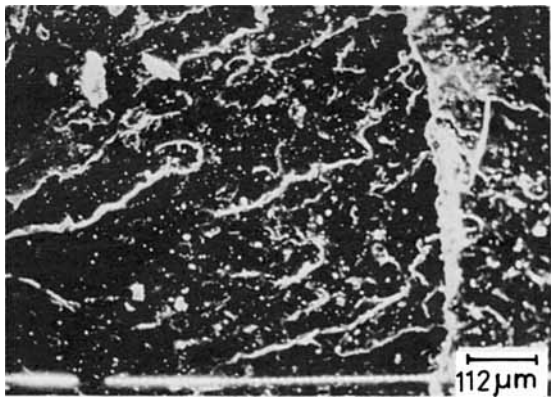

Fig. 7. SEM photomicrograph of the tensile-fractured surface of mix G.

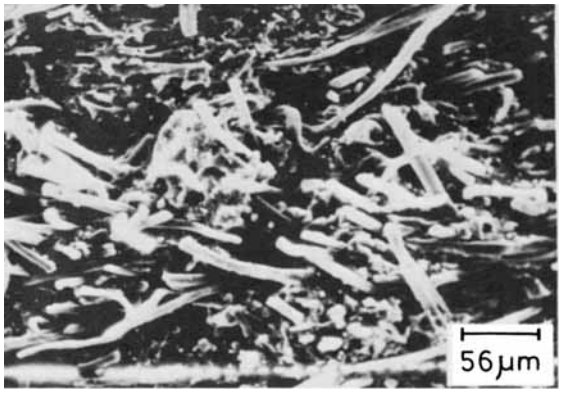

Fig. 8. SEM photomicrograph of the tensile-fractured surface of mix D with longitudinal fiber orientation.

cracks over the fracture surface, as shown in Figure 8, which is the SEM photomicrograph of the tensile fractured surface of mix D with longitudinal fiber orientation. The high level of fiber–rubber adhesion in this case causes breakage of the fibers without pulling them out of the rubber matrix. In the transverse orientation, as expected, fiber breakage and pulling out become insignificant (Fig. 9). This accounts for the lower tensile strength of mix D in this orientation compared to that in the longitudinal orientation.

Swelling in chloroform is restricted to a pronounced degree due to addition of fibers in the mixes, as evident from Table V. Higher V_r value for mix D compared to that for mix F signifies greater fiber–rubber adhesion.

Stiffness of the vulcanizates increases on the addition of fibers to the mixes. Hence fiber-filled mixes D and F show a lower compression set at constant stress than unfilled mix G. As expected, lower values of the compression set at constant stress were observed for the samples with longitudinal fiber orientation than for the samples with transverse fiber orientation.

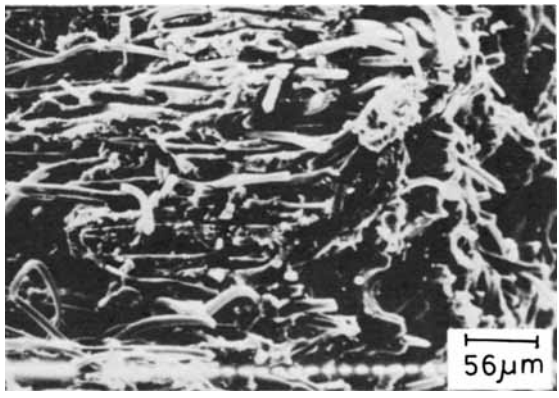

Fig. 9. SEM photomicrograph of the tensile-fractured surface of mix D with transverse fiber orientation.

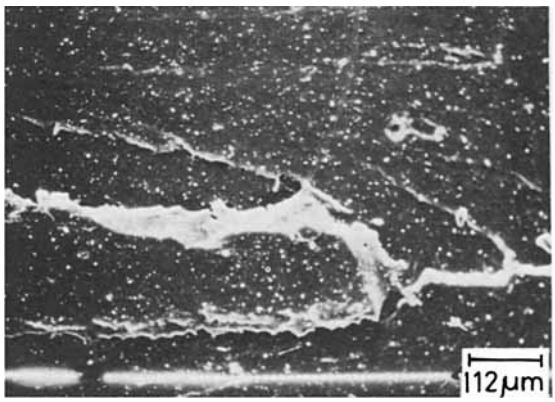

Fig. 10. SEM photomicrograph of the tear-fractured surface of mix G.

Compression set at constant strain, however, shows an opposite trend. In this case greater stiffness requires higher applied load to maintain 25% strain in the samples. Mixes D and F show, therefore, higher compression set compared to mix G, and higher values are obtained in the longitudinal fiber orientation than in the transverse fiber orientation. However, better fiber–matrix adhesion in mix D as compared to that in mix F leads to lower compression set in the former.

An increase in hardness and decrease in resilience was observed due to the presence of fibers in the mixes. Mix D, as expected, showed higher hardness and better resilience compared to mix F.

A remarkable improvement in tear strength is observed when fibers are present in the mixes. With longitudinal fiber orientation mixes D and F show approximately the same tear strength due to equal concentration of fibers in the mixes. While in the transverse fiber orientation, higher tearing energy as a result of better fiber–rubber adhesion causes higher tear strength for mix D compared to that for mix F.

SEM photomicrograph of the tear-fractured surface of the unfilled vul-

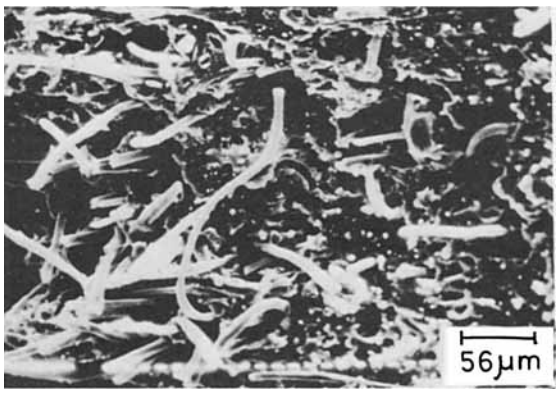

Fig. 11. SEM photomicrograph of the tear-fractured surface of mix D with longitudinal fiber orientation.

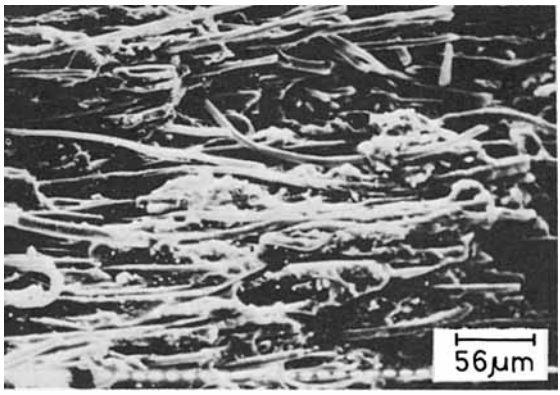

Fig. 12. SEM photomicrograph of the tear-fractured surface of mix D with transverse fiber orientation.

canizate of mix G is shown in Figure 10. It shows the presence of steady tear lines along with a thick tear path on a relatively smooth fracture surface. Formation of cracks at the end of this tear path is also observed. The presence of fibers in the mixes altogether changes the failure mode. Figure 11 shows the SEM photomicrograph in tear-fractured surface of mix D with longitudinal fiber orientation. Breakage of fibers and formation of cracks and grooves are the characteristics of this fractograph. In the case of transverse fiber orientation, however, the fracture path moves parallel to the direction of orientation of fibers (Fig. 12) and fiber breakage does not occur.

Increased stiffness due to the addition of fibers in mixes D and F compared to that in the non-fiber-filled mix G requires the application of a higher mechanical stress on the test specimens in Goodrich flexometer testing in order to maintain constant strain in all cases. Higher heat buildup for the mixes D and F in both fiber orientations than for mix G is, therefore, observed. In the transverse orientation, however, the number of fibers pulled out is more, and consequent frictioning among them leads to higher

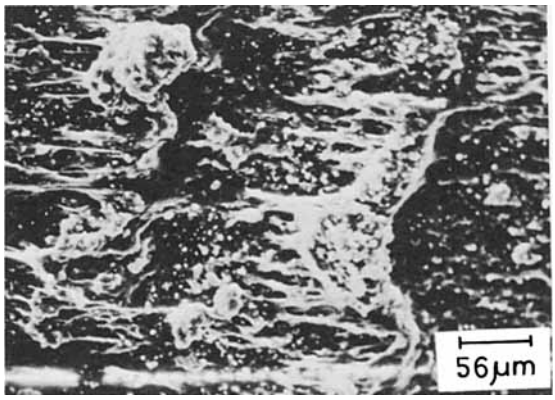

Fig. 13. SEM photomicrograph of the abraded surface of mix G.

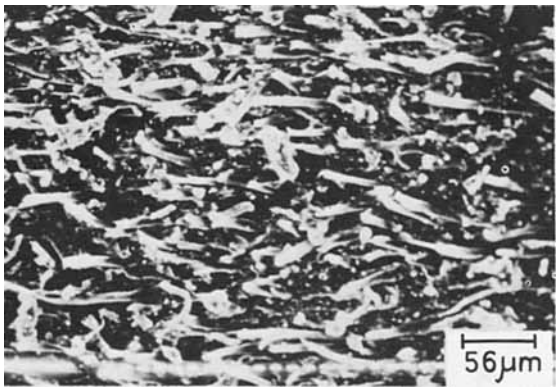

Fig. 14. SEM photomicrograph of the abraded surface of mix D with longitudinal fiber orientation.

temperature rise. This is similar to our earlier observation in the case of short silk fiber–nitrile rubber composites.[32] Lower fiber–matrix adhesion in mix F causes failure of the test specimens at an earlier stage than in mix D.

Abrasion properties improve significantly in the fiber-filled mixes D and F unlike in mix G. Abrasion loss is found to be less when the fibers are oriented perpendicular to the counterface (transverse orientation) than when they are oriented parallel to the sliding surface (longitudinal orientation). This observation is similar to the earlier observations.[32,39,40] Mix D, in both the orientations, shows better abrasion resistance than mix F.

Figure 13 is the SEM photomicrograph of the abraded surface of unfilled vulcanizate of mix G. It shows extensive material displacement from left to right which is also the direction of applied frictional force experienced by the specimen surface when sliding against the abrasive wheel. Channels produced as a result of this material removal are bridged by fibrils. Figure 14 is the SEM photomicrograph of the abraded surface of mix D with lon-

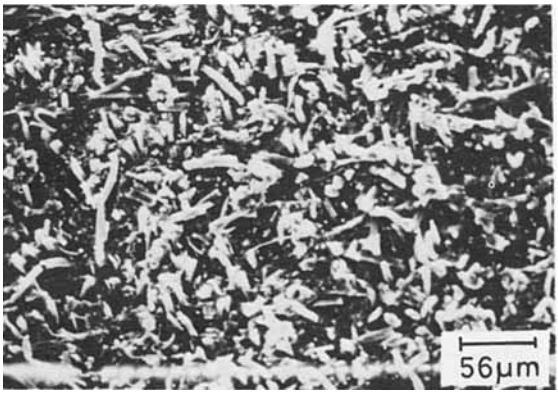

Fig. 15. SEM photomicrograph of the abraded surface of mix D with transverse fiber orientation.

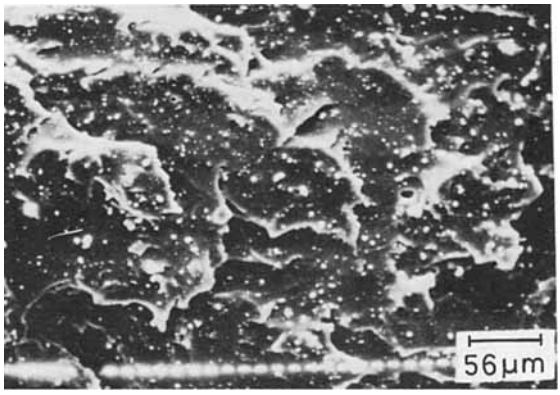

Fig. 16. SEM photomicrograph of the flex-failed surface of mix G.

gitudinally oriented fibers. It shows orientation of the fibers parallel to the sliding direction and the formation of grooves on the fracture surface. In the transverse orientation (Fig. 15), bending and breakage of fibers are evident. The extra work necessary to bend and break the fibers is responsible for the higher wear resistance exhibited by the composites in this orientation.

Addition of fibers in mixes D and F deteriorates the flex cracking resistance. Longitudinal orientation of fibers registers higher stiffness in the direction of flexing, which leads to poorer flex cracking resistance than that in the transverse orientation.

SEM photomicrograph of flex-failed surface of the gum mix G (Fig. 16) shows brittle failure with extensive cracking over the fracture surface, thus supporting the experimental observation of a low flex cracking resistance in this case. The SEM photomicrograph of the flex-failed surface of mix D with longitudinal fiber orientation (Fig. 17) shows local buckling of the fibers because of repeated flexing of the test specimens in the De Mattia flexometer testing. Successive bucklings of adjacent layers of fibers cause

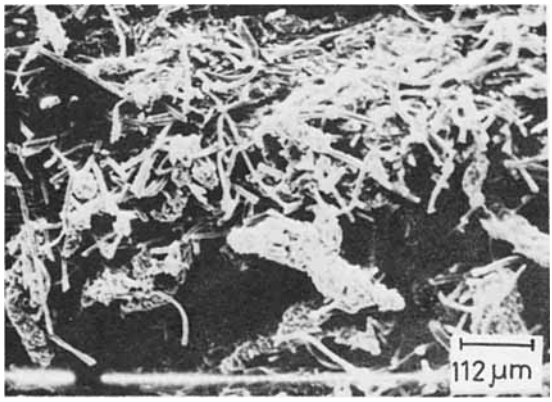

Fig. 17. SEM photomicrograph of the flex-failed surface of mix D with longitudinal fiber orientation.

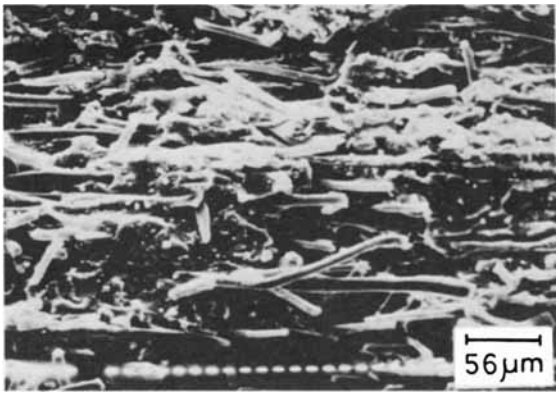

Fig. 18. SEM photomicrograph of the flex-failed surface of mix D with transverse fiber orientation.

extensive breakage of fibers and lead to the development of deep cracks and cavities over the fracture surface due to removal of rubber masses agglomerated with the broken fibers. In transverse orientation of this mix (Fig. 18), fiber buckling and removal of rubber masses with adhering broken fibers are not observed because of the propagation of the fracture in the direction of fiber orientation. Higher flex cracking resistance in this orientation than that in the longitudinal orientation is, therefore, observed.

Processing Characteristics

The presence of fibers in the mixes affects the processing characteristics significantly, as observed in Table VI. Addition of fiber in the compounds (mixes D and F) increases green strength both in the longitudinal and transverse orientation as compared to mix G (without fiber). Mill shrinkage also reduces drastically in mixes D and F. However, the Mooney viscosity ML (1 + 4) increases on the addition of fibers and is maximum in the case of silica containing mix D containing silica–cohedur bonding system. Moo-

TABLE VI
Processing Characteristics of the Mixes

Property	Fiber orientation	Mix D (cohedur–silica bonding system)	Mix F (cohedur–carbon black bonding system)	Mix G (without fiber and bonding agents)
Mill shrinkage (%)	—	2.0	1.5	56.0
Mooney viscosity ML (1 + 4), at 120°C	—	49.5	37.0	27.0
Mooney scorch time T_5 at 120°C (min)	—	11.5	10.5	28.0
Green strength (MPa)	L	2.72	3.25	—
	T	0.55	0.49	

ney scorch time, however, decreases sharply due to the addition of both bonding agents and fibers in the mixes, and mix F shows the lowest scorch safety.

The authors are thankful to Professor S. K. De of Rubber Technology Centre, I. I. T., Kharagpur for helpful discussions. One of the authors (D. K. S.) is thankful to the National Council of Educational Research and Training, New Delhi, for financial assistance.

References

1. A. Y. Coran, P. Hamed, and L. A. Goettler, *Rubber Chem. Technol.*, **49**, 1167 (1976).
2. K. Boustany and R. L. Arnold, *J. Elastoplast.*, **8** 160 (1976).
3. B. E. Brokenbrow, D. Simes, and A. G. Stokoe, *Rubber J.*, **151**, 51 (1969).
4. G. C. Derringer, *J. Elastoplast.*, **3**, 230 (1971).
5. J. E. O'Connor, *Rubber Chem. Technol.*, **50**, 945 (1977).
6. A. Y. Coran, K. Boustany, and P. Hamed, *Rubber Chem. Technol.*, **47**, 396 (1974).
7. A. Y. Coran, K. Boustany, and P. Hamed, *J. Appl. Polym. Sci.*, **15**, 2471 (1975).
8. S. K. Chakraborty, D. K. Setua, and S. K. De, *Rubber Chem. Technol.*, **55**, 1286 (1982).
9. V. M. Murty and S. K. De, *Rubber Chem. Technol.*, **55**, 287 (1982).
10. L. A. Goettler, R. I. Leib, and A. J. Lambright, *Rubber Chem. Technol.*, **52**, 838 (1979).
11. L. A. Goettler, A. J. Lambright, R. I. Leib, and P. J. Dimauro, *Rubber Chem. Technol.*, **54**, 277 (1981).
12. L. A. Goettler, R. I. Leib, P. J. Dimauro, and K. E. Kear, paper presented at the fall Technical Seminar of the Detroit Rubber Group, October 1979.
13. J. R. Beatty and P. Hamed, paper presented at the ACS Meeting, Rubber Div., Montreal, Quebec, Canada, May 1978.
14. J. W. Rogers and D. W. Carlson, paper presented at the ACS Meeting, Rubber Div., Minneapolis, Minnesota, April 1976.
15. Patent to Bridge Stone Co., Chem. Abstr., **96**, 219182f (1982).
16. Patent to Armstrong Cork Co., *Chem. Abstr.*, **83**, 207423f (1975).
17. Hi-Sil Bulletin No. 40, Chemical Division, PPG Industries, Inc., Pittsburgh, August 1969.
18. Y. Takagi and S. Tada, Nippon Gomu Kyokaishi, No. 2, 118 (1981); *Int. Polym. Sci. Technol.*, **8**(10), 59 (1981).
19. T. N. Nesiolovskaya, E. M. Solov'ev, N. D. Zakharov, D. P. Emel'yanov, N. L. Sergeeva, and G. M. Galybin, *Int. Polym. Sci. Technol.*, **10**(3), 73 (1983).
20. Anonymous, *Gummi Asbest Kunstst.*, **35**(10), 552 (1982); *Int. Polym. Sci. Technol.*, **10**(2), 35 (1983).
21. E. A. Dzyura, A. V. Kuz'min, L. G. Klimenko, and V. N. Belkovskii, *Kauch Rezina*, No. 12, 27 (1982); *Int. Polym. Sci. Technol.*, **10**(4), 1 (1983).
22. E. M. Solov'ev, I. A. Kuznetsova, N. M. Levkina, and N. D. Zakharov, *Int. Polym. Sci. Technol.* **7**(5), 16 (1980).
23. A. Kuznetsova, E. M. Solov'ev, N. D. Zakharov, Yu. N. Gorodnichev, and G. L. Malakhova, *Int. Polym. Sci. Technol.*, **7**(6), 15 (1980).
24. E. M. Solov'ev, E. M. Borisov, N. D. Zakharov, G. M. Galybin, D. P. Emel'yanov, N. L. Sergeeva, and V. M. Baikov, *Int. Polym. Sci. Technol.*, **7**(9), 69 (1980).
25. L. A. Goettler and K. S. Shen, paper presented at the ACS Meeting, Rubber Div., Chicago, October 1982.
26. J. M. Campbell, *Prog. Rubber Technol.*, **41**, 43 (1978).
27. Technical Report No. 34, Rubber Chemicals Div., Monsanto Co., Louvian-La Neuve, Belgium.
28. Technical Report No. 31, Rubber Chemicals Div., Monsanto Co., Louvian-La Neuve, Belgium.
29. F. Manceau, *Rev. Gen. Caoutch. Plast.*, **95**, 542 (1979).
30. G. C. Derringer, *Rubber World*, **165**, 45 (1971).
31. D. K. Setua and S. K. De, *Rubber Chem. Technol.*, **56**, 808, (1983).
32. D. K. Setua and S. K. De, *J. Mater. Sci.*, **19**, 983 (1984).
33. J. R. Creasey and M. P. Wagner, *Rubber Age*, **100**, 72 (1968).
34. N. L. Hewitt, *Rubber Age*, **104**, 59 (1972).

35. E. Morita, *Rubber Chem. Technol.*, **53**, 795 (1980).
36. V. M. Murty and S. K. De, *J. Appl. Polym. Sci.*, **27**, 4611 (1982).
37. B. Das, *J. Appl. Polym. Sci.*, **17**, 1019 (1973).
38. D. K. Setua and S. K. De, *J. Mater. Sci.*, **18**, 847 (1983).
39. Z. Eliezer, V. D. Khanna, and M. F. Amatenu, *Wear*, **53**, 387 (1979).
40. Nak-Ho Sung and Nam P. Suh, *Wear*, **53**, 129 (1979).

Received November 28, 1983
Accepted January 25, 1984